

Thermal properties of carbon nanotubes and nanotube-based materials

J. Hone^{1,*}, M.C. Llaguno¹, M.J. Biercuk¹, A.T. Johnson¹, B. Batlogg², Z. Benes³, J.E. Fischer³

¹ Department of Physics and Astronomy and Laboratory for Research on the Structure of Matter, University of Pennsylvania, Philadelphia PA 19104-6272, USA

² Bell Laboratories, Lucent Technologies, Murray Hill, NJ 079743, USA

³ Department of Materials Science and Engineering and Laboratory for Research on the Structure of Matter, University of Pennsylvania, Philadelphia PA 19104-6272, USA

Received: 17 October 2001/Accepted: 3 December 2001/Published online: 4 March 2002 – © Springer-Verlag 2002

Abstract. The thermal properties of carbon nanotubes are directly related to their unique structure and small size. Because of these properties, nanotubes may prove to be an ideal material for the study of low-dimensional phonon physics, and for thermal management, both on the macro- and the micro-scale. We have begun to explore the thermal properties of nanotubes by measuring the specific heat and thermal conductivity of bulk SWNT samples. In addition, we have synthesized nanotube-based composite materials and measured their thermal conductivity.

The measured specific heat of single-walled nanotubes differs from that of both 2D graphene and 3D graphite, especially at low temperatures, where 1D quantization of the phonon bandstructure is observed. The measured specific heat shows only weak effects of intertube coupling in nanotube bundling, suggesting that this coupling is weaker than expected. The thermal conductivity of nanotubes is large, even in bulk samples: aligned bundles of SWNTs show a thermal conductivity of > 200 W/m K at room temperature. A linear $K(T)$ up to approximately 40 K may be due to 1D quantization; measurement of $K(T)$ of samples with different average nanotube diameters supports this interpretation.

Nanotube-epoxy blends show significantly enhanced thermal conductivity, showing that nanotube-based composites may be useful not only for their potentially high strength, but also for their potentially high thermal conductivity.

PACS: 62.25.+g; 63.22.+m; 61.46.+w

1 Specific Heat

A carbon nanotube can be thought of as a single graphene sheet that is wrapped into a cylinder. Wrapping the sheet has two major effects on the phonon bandstructure. Firstly, the 2D

phonon bandstructure of the sheet “folds” into the 1D bandstructure of the tube. Secondly, the cylindrical shape of the tube renders it stiffer than the sheet, changing the dispersion of the lowest-lying modes.

Figure 1 shows the theoretically derived low-energy phonon bandstructure of an isolated (10, 10) nanotube [1]. The 1D quantized nature of the bandstructure is evident: there are a series of 1D “sub-bands” separated at the zone center by energies of a few meV. There are four acoustic bands; one longitudinal (LA), two degenerate transverse (TA), and one “twist”, all of which have linear dispersion at low energy. The high phonon band velocity ($v_{LA} = 24$ km/s, $v_{TA} = 15$ km/s,

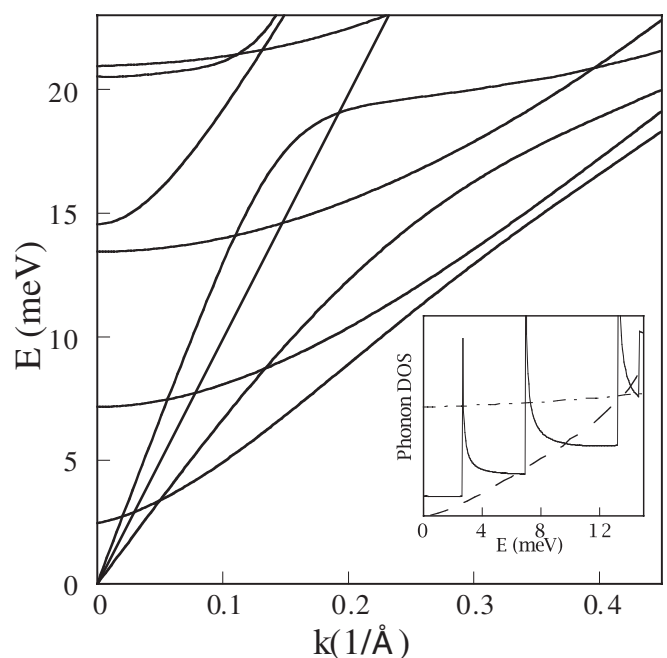


Fig. 1. Low-energy phonon bandstructure of a (10, 10) carbon nanotube [1]. The inset shows the phonon density of states (PDOS) of an isolated nanotube (solid line) compared to the PDOS of graphene (dot-dashed line) and graphite (dashed line)

*Corresponding author.

Present address: Department of Physics, California Institute of Technology, Pasadena CA 91125, USA

(Fax: +1-626/683-9060, E-mail: hone@caltech.edu)

$v_{\text{twist}} = 9 \text{ km/s}$), coupled with the small diameter of the nanotube, causes the relatively large sub-band splitting.

The inset shows the low-energy phonon density of states (PDOS) of a (10, 10) nanotube (solid line) compared to that of 2D graphene (dot-dashed line) and 3D graphite (dashed line). The nanotube PDOS is constant at the lowest energies, and then increases stepwise with the entry of higher subbands. As the system is 1D, there is a van Hove singularity at each band edge. The graphene PDOS is large in this energy range because of the existence of an out-of-plane transverse mode with quadratic dispersion. The PDOS of graphite, however, is significantly reduced because of the added coupling between neighboring layers, which renders the system 3D rather than 2D, and shifts low-energy spectral weight upward in energy.

Figure 2 shows the calculated low-temperature heat specific heat of an isolated nanotube. Because the PDOS is constant at low energy, the specific heat displays linear temperature dependence at low temperature because only the acoustic modes are populated [2]. Above $\sim 6 \text{ K}$, the slope of $C(T)$ increases as the optical sub-bands become populated. This linear behavior, with an increase in slope near 6 K , is the expected signature for a 1D quantized phonon spectrum in single-walled nanotubes.

As can be seen in the case of graphene and graphite, changing the dimensionality of a system can greatly affect the low-energy PDOS and therefore the low-temperature specific heat. In graphite, the range of this effect is related to the Debye energy of the interlayer modes, approximately 10 meV . In nanotubes, it might be expected that bundling tubes into 3D crystalline arrays (“ropes”) would reduce the low-energy PDOS. Mizel et al. [3] have calculated the low-energy phonon bandstructure of SWNT bundles, and find a relatively high intertube Debye energy E_D^\perp , approximately 5 meV , for the case where neighboring tubes have graphite-like (“strong”) coupling.

Figure 3 shows the predicted specific heat of 2D graphene, 3D graphite, 1D isolated SWNTs and 3D SWNT ropes, showing the dramatic effects of differing interlayer coupling. At high temperatures, all of the specific heats are identical and mostly reflect the phonon structure of the constituent 2D

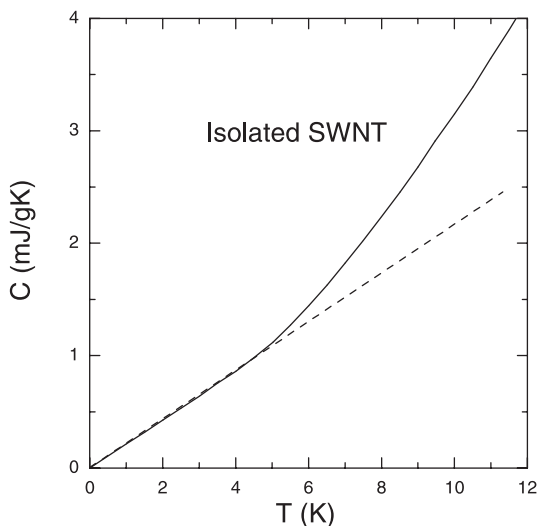


Fig. 2. Calculated single-nanotube specific heat

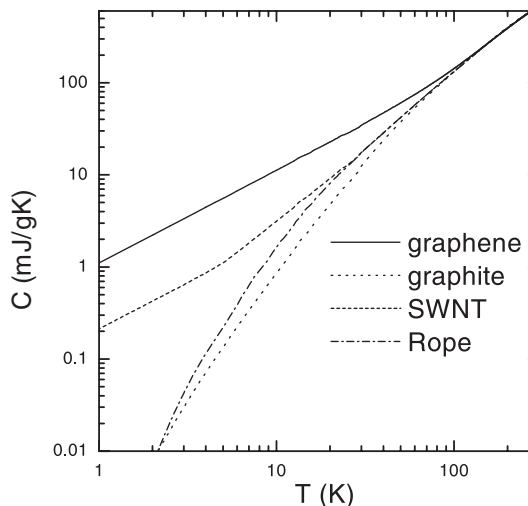


Fig. 3. Predicted specific heat of a graphene sheet, an isolated nanotube, graphite, and a nanotube rope

graphene sheets. Comparing 2D graphene to 3D graphite, we can see that below approximately 60 K , interlayer coupling causes $C(T)$ to decrease much more strongly with temperature. The isolated SWNT displays a smaller $C(T)$ at low temperature compared to the graphene sheet due to the absence of the quadratic out-of-plane mode-tubes, which are stiffer to bending than sheets. Finally, the strongly coupled rope curve diverges below the single-tube $C(T)$ below 30 K , following a curve similar to that of graphite. It is clear from Fig. 3 that graphite-like coupling between neighboring tubes in a SWNT bundle should cause the signature of 1D quantization in the specific heat to be obscured. However, in the case of weaker coupling, single-tube behavior might persist to lower temperatures.

The SWNT samples used for measurement of specific heat [4] were obtained from purified SWNT suspensions (tubes@rice), and subsequently purified and vacuum-annealed. The sample was composed of large bundles of SWNTs with an average tube diameter of 1.25 nm and the residual catalyst concentration was approximately 2 at. \% , as determined by X-ray diffraction (XRD), high-resolution transmission electron microscopy (HRTEM) and energy-dispersive X-ray spectroscopy (EDX) measurements. After analysis, the samples were baked at 300°C under dynamic vacuum for three days to remove atmospheric contaminants, and then kept under vacuum until minutes before the measurements were begun. Specific heat was measured from 300 K to 2 K using a relaxation technique.

Figure 4 shows the measured specific heat of a SWNT sample from 2 K to 300 K . The hollow circles represent the raw data. The solid line represents the contribution from the catalyst, based on the known specific heat of Ni and Co. Finally, the solid circles represent the corrected specific heat of the SWNTs. Figure 5 shows the measured specific heat on a logarithmic scale, compared to the predicted specific heat of graphene, graphite, isolated SWNTs and strongly coupled ropes. The measured data follows the isolated SWNT curve all the way down to 4 K . Thus, existing models of the phonon bandstructure of SWNTs are largely consistent with the measured data. The data diverge below the single-tube curve at 4 K , rather than at 30 K , as expected for the case of graphite-

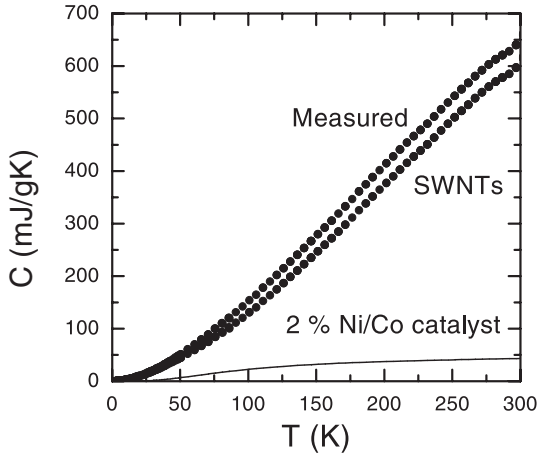


Fig. 4. Measured specific heat of a purified SWNT sample [4]. The raw data is corrected for the contribution from the catalyst impurities to obtain the contribution from the SWNTs

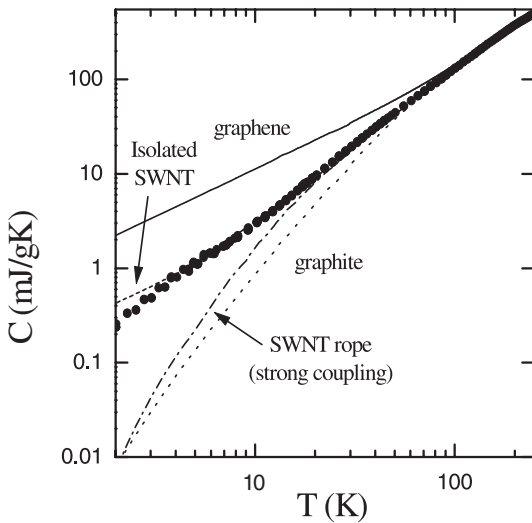


Fig. 5. Measured specific heat compared to theoretical models [4]. The data agree with the predicted $C(T)$ of an isolated nanotube down to 4 K, implying a weak intertube interaction

like coupling. Therefore, we conclude that SWNTs are much more weakly coupled mechanically than might be expected; it should be possible to observe the 1D–2D transition characteristic of single tubes.

The solid points in Fig. 6 show the low-temperature measured specific heat on a linear scale. The data clearly show a linear temperature dependence from 2 K to 8 K, with an increase in slope above 8 K. This behavior is direct confirmation of a 1D-quantized phonon spectrum in SWNTs. However, the linear slope does not extrapolate to zero at $T = 0$, as would be expected for isolated SWNTs. We attribute this discrepancy to intertube coupling, which should cause T^3 -like behavior at low temperature.

The lines in Fig. 6 show the results of employing a simple model to simulate the behavior of weakly coupled SWNT ropes. In this model, the acoustic modes are collapsed onto a single mode with Debye energy E_D^{\parallel} in the on-tube direction, and transverse Debye energy E_D^{\perp} , with a specific heat represented by the dashed line. A single optical mode enters at E_{sub} , with specific heat represented by the

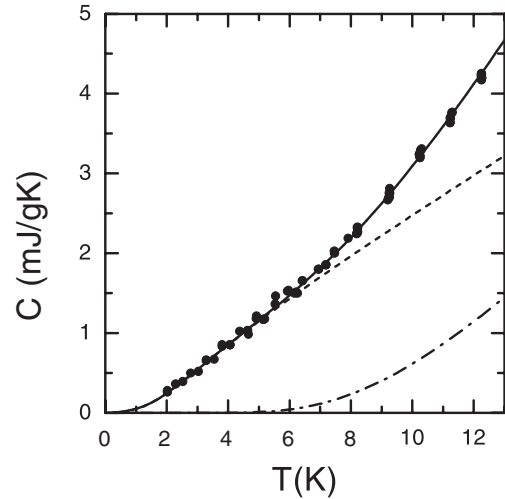


Fig. 6. Measured specific heat at low temperature; fit using a simple model to account for weak intertube interactions [4]

dot-dashed line; the solid line represents the sum of the two contributions. E_D^{\parallel} , E_D^{\perp} , and E_{sub} are taken as independent fitting parameters, and adjusted to give the best fit to the measured data. The values obtained are $E_D^{\parallel} = 92$ meV, $E_D^{\perp} = 1.4$ meV, and $E_{\text{sub}} = 4.1$ meV.

The theoretical acoustic mode velocities for a SWNT [1] translate into an effective Debye energy of 103 meV, only slightly higher than the fitted 92 meV. Our fitted E_{sub} (4.1 meV), however, is considerably larger than the theoretical single-tube value of 2.7 meV. The first optical sub-band corresponds to tube flattening, and should require significantly more energy in a rope since tubes are constrained by their neighbors; theoretical calculations [5] that take radial tube-tube interactions into account show excellent agreement with the experimental value. The experimental tube–tube coupling, measured by $E_D^{\perp} = 1.2$ meV, is significantly smaller than the theoretical value of approximately 5 meV [3] obtained using coupling constants derived from graphite. The difference may be related to the lack of commensurability between neighboring tubes, which would imply a dramatic weakening of the corrugation in the intertube potential, so that tubes in a real rope may slide or twist more freely than expected.

The measured high on-tube Debye energy confirms, in a bulk sample, the high Young's modulus previously observed for individual tubes [6]. The weak tube–tube coupling, however, implies that the mechanical strength of SWNT ropes will be relatively poor. It may be necessary to crosslink tubes within a rope, or to separate them completely, in order to realize their near-ideal properties in high-strength composites. However, weak coupling may be an advantage for high thermal conductivity. Berber et al. [7] find that strong tube–tube coupling decreases the high-temperature thermal conductivity of SWNT bundles by an order of magnitude relative to isolated tubes; weak coupling may imply no significant reduction in the thermal conductivity when tubes are bundled into ropes. Similarly, in composites, the inner tubes in a rope should be relatively unperturbed by the surrounding matrix, which could also be an advantage for high thermal conductivity. The issues of commensurability that were raised as an explanation for the weak tube–tube mechanical coupling also

have implications for the electronic coupling between neighboring SWNTs in a rope [8].

2 Thermal conductivity

As diamond and graphite display the highest known thermal conductivity at moderate temperatures, it is likely that nanotubes should be outstanding in this regard as well. Indeed, recent theoretical work [7] has predicted that the room-temperature thermal conductivity of nanotubes is as high as 6600 W/m K . In addition, at low temperature, the thermal conductivity should show the effects of 1D quantization just as is seen in the specific heat. The thermal conductivity in a highly anisotropic material is most sensitive to the high-velocity and high-scattering-length phonons. Therefore, it is likely that even in nanotube bundles, the thermal conductivity should directly probe on-tube phonons and be insensitive to inter-tube coupling.

Figure 7 shows the measured temperature-dependent thermal conductivity of bulk samples of SWNTs that have been aligned by filtration in a high magnetic field [9]. In the alignment direction, the room-temperature thermal conductivity is greater than 200 W/m K , which is comparable to a good metal and within an order of magnitude of that of highly crystalline graphite or diamond. The thermal conductivity of unaligned samples is about one order of magnitude smaller [10]. However, the temperature dependence of the thermal conductivity is roughly the same in both types of sample. Also, in both types of sample, simultaneous measurement of the electrical and thermal conductivity shows that the electronic contribution to $K(T)$ is negligible at all temperatures.

Below approximately 40 K, the thermal conductivity displays a strictly linear temperature dependence in all samples. This temperature dependence is likely to be due to 1D quan-

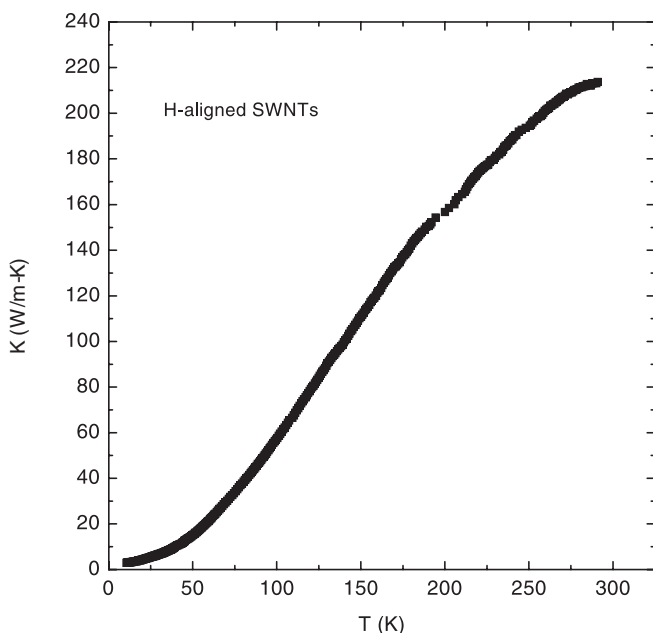


Fig. 7. Thermal conductivity of a bulk sample of SWNTs in which the tubes are aligned by filtration in a strong magnetic field [9]. The measurement is taken in the direction parallel to the tubes

tization, in which only the acoustic modes of the tube carry any heat flow. However, the role of intertube contacts on the temperature dependence of $K(T)$ is unknown. In order to more definitively determine whether the linear $K(T)$ is due to 1D quantization, we have measured $K(T)$ for samples with different nanotube diameters. Because the phonon sub-band splitting increases with decreasing tube diameter, we expect that the linear $K(T)$ should extend to higher temperatures in samples with a smaller average tube diameter.

Figure 8 shows the thermal conductivity divided by temperature, $K(T)$, for four SWNT samples [11]. The samples were synthesized by laser ablation at differing oven temperatures in order to produce different average nanotube diameters. Two samples synthesized at 1100°C , with an average diameter of 1.4 nm, and two samples synthesized at 1200°C , with an average diameter of 1.2 nm, were measured. All four samples show a linear $K(T)$ at low temperature, as shown by the constant value of K/T (normalized to 1 here for all samples). For the 1.4 nm diameter samples (open symbols), K/T begins to increase at approximately 35 K, while a similar increase is not seen for the 1.2 nm samples (filled symbols) until approximately 40 K. This behavior is consistent with our expectations for a 1D quantized thermal conductivity. A puzzling inconsistency, however, is that the linear $K(T)$ extends to approximately 40 K while the linear $C(T)$ extends only to approximately 8 K. If the phonon scattering time is relatively constant for all modes, these temperatures should be roughly equal. One possible explanation for this discrepancy is that the optical sub-bands of the nanotube scatter much more strongly than the acoustic sub-bands, so that their influence on the thermal conductivity is suppressed until higher temperatures are reached. Clearly, more experimental and theoretical work is necessary in order to fully understand this behavior.

Composite materials having high thermal conductivity have a number of potential applications, particularly in heat sinking for electronics and motors. To explore the potential

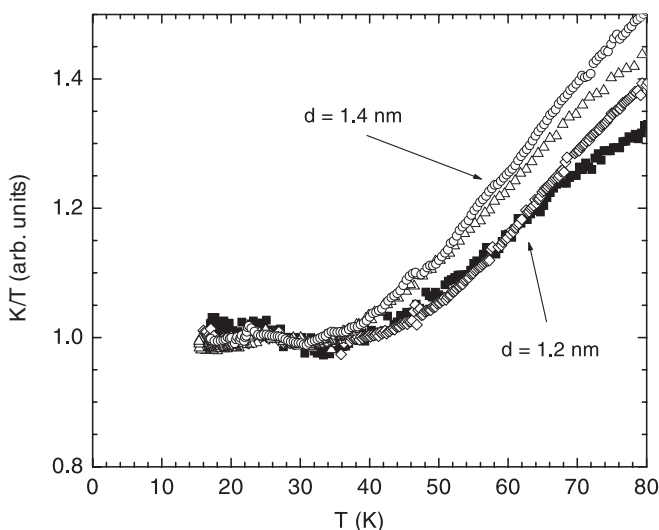


Fig. 8. Thermal conductivity divided by temperature, $K(T)$, of SWNT samples with different average diameters [11]. The range of linear $K(T)$, i.e. constant K/T , extends to higher temperatures in samples with a smaller diameter, as would be expected for a scenario of 1D quantization of the phonon structure

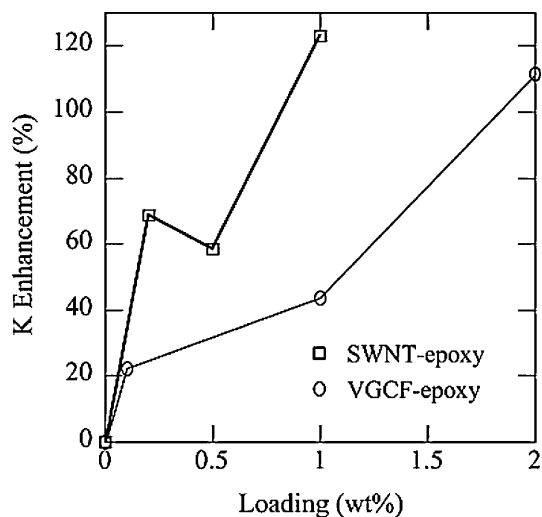


Fig. 9. Thermal conductivity enhancement for epoxy samples with varying loading of SWNTs and vapor-grown carbon fibers (VGCF) [12]

of using nanotubes for such applications, we have synthesized nanotube-based composites by mixing as-grown nanotube soot into industrial epoxy (Shell Chemicals Epon 862 epoxy resin) [12]. As a comparison, highly graphitic vapor-grown carbon fibers (VGCF) were mixed into the same resin. Figure 9 shows the measured room-temperature thermal conductivity enhancement for samples with 0–1 wt % nanotubes, and 0–2 wt % VGCF. The nanotube samples show an increasing thermal conductivity enhancement with increasing load-

ing, with a 120% enhancement at 1% loading. In addition, nanotubes seem to be superior to VGCF as a filler material. This initial result demonstrates that nanotubes are, in fact, an excellent filler for making high-thermal-conductivity composites.

Acknowledgements. This work was supported by NSF Grant No. DMR-9802560, DOE Grant No. DEFG02-98ER45701 and the Laboratory for Research on the Structure of Matter MRSEC, No. DMR00-79909.

References

1. R. Saito, G. Dresselhaus, M.S. Dresselhaus: *Physical Properties of Carbon Nanotubes* (Imperial College Press, London 1998)
2. L.X. Benedict, S.G. Louie, M.L. Cohen: *Solid State Comm.* **100**, 177 (1996)
3. A. Mizel, L.X. Benedict, M.L. Cohen, S.G. Louie, A. Zettl, N.K. Budraa, W.P. Beyermann: *Phys. Rev. B* **60**, 3264 (1999)
4. J. Hone, B. Batlogg, Z. Benes, A.T. Johnson, J.E. Fischer: *Science* **289**, 1730 (2000)
5. D. Kahn, J.P. Lu: *Phys. Rev. B* **60**, 6535 (1999)
6. W. Teizer, R.B. Hallock, E. Dujardin, T.W. Ebbesen: *Phys. Rev. Lett.* **82**, 5305 (1999)
7. S. Berber, Y.K. Kwon, D. Tomaneck: *Phys. Rev. Lett.* **84**, 4613 (2000)
8. A.A. Maarouf, C.L. Kane, E.J. Mele: *Phys. Rev. B* **61**, 11 156 (2000)
9. J. Hone, M.C. Llaguno, N.M. Nemes, A.T. Johnson, J.E. Fischer, D.A. Walters, M.J. Casavant, J. Schmidt, R.E. Smalley: *Appl. Phys. Lett.* **77**, 666 (2000)
10. J. Hone, M. Whitney, C. Piskoti, A. Zettl: *Phys. Rev. B* **59**, R2514 (1999)
11. M.C. Llaguno, J. Hone, J.E. Fischer, A.T. Johnson: in press
12. M.J. Biercuk, M.C. Llaguno, M. Radosavljevic, J.K. Hyun, A.T. Johnson, J.E. Fischer: in press